Heterogeneous Catalysis

DOI: 10.1002/anie.201410016

Impact of Pore Connectivity on the Design of Long-Lived Zeolite Catalysts**

*Maria Milina, Sharon Mitchell, David Cooke, Paolo Crivelli, and Javier Pérez-Ramírez**

Abstract: *Without techniques sensitive to complex pore architectures, synthetic efforts to enhance molecular transport in zeolite and other porous materials through hierarchical structuring lack descriptors for their rational design. The power of positron annihilation lifetime spectroscopy (PALS) to characterize the pore connectivity in hierarchical MFI zeolites is demonstrated, establishing a direct link with the enhanced catalyst lifetime in the conversion of methanol to valuable hydrocarbons. The unique ability to capture subtleties of the hierarchical structure originates from the dynamic nature of the ortho-positronium response to the pore network. The findings reveal the strong dependence on the way in which the hierarchical zeolites are manufactured, having direct implications for the practical realization of these advanced catalysts.*

Complex porous materials are pivotal in the development of many cutting-edge technologies, the pore network typically balancing the efficiency of a physical process with specific chemical functions.[1] Hierarchically structured zeolite catalysts are an elegant example of systems in which the introduction of an auxiliary network of meso- and/or macropores to facilitate molecular transport to the active sites located in the micropores yields enhanced performance in numerous hydrocarbon transformations.[2] To optimize the design of such materials, it is imperative to correlate the pore topology, determined by the amount, size, connectivity, and distribution of each porosity level, with the catalytic impact. This requires both techniques sensitive to relevant pore characteristics and the availability of materials with comparable bulk properties, but differing pore topology. One of the most powerful methods to assess the pore structure is undoubtedly the direct visualization by transmission electron tomography, which has enabled the derivation of the tortuosity and accessibility of mesopores within individual zeolite crystals.[3] Over a wider range of length scales, such as those spanned in technical zeolite bodies, integrated imaging approaches coupled with dedicated sample preparation become necessary.[4] Indirect methods, such as hyperpolarized ^{129}Xe or pulsed field gradient (PFG-) NMR, have also attracted interest to study the interconnectivity of the micro- and mesopores.[5] However, to date none of the parameters derived have been quantitatively correlated with the catalytic performance.

By introducing a top-down demetalation strategy to develop distinct open or constricted mesopore configurations in MFI-type crystals, we recently exposed the major impact of pore architecture on the lifetime of the hierarchical zeolites in the conversion of methanol to hydrocarbons (MTH).[6] The dissimilar pore structures of these model catalysts could be readily distinguished by gas sorption, mercury porosimetry, identical-location scanning transmission and secondary electron microscopy, and positron annihilation lifetime spectroscopy (PALS). Yet, to really push the performance and economic boundaries of zeolite catalysts, a much more precise understanding of the role of the hierarchical pore network is required in relevant platforms of materials. Here, taking desilication as a highly scalable and versatile manufacturing method,[7] we have followed different approaches altering the concentration ($x = 0.05$–0.3 M NaOH) and duration ($y = 5$–30 min) of alkaline treatment to prepare a matrix of hierarchical zeolites (ATx-y) of widely differing mesoporosity, depending on the extent of dissolution (Table 1). Comparatively, as shown in the same table, the acidic properties of the samples vary within a very narrow range.

Evaluation of the hierarchical zeolites in the MTH reaction (Figure 1) confirms large differences in the cycle time, defined as the time for which the conversion exceeds 95%, which is extended by between 1.3–3.6 times that of the conventional analogue (C). Only minor variations in the average product selectivity to light olefins ($S_{C2–C4\ olefins} = 40 \pm 2$ Cmol%) or aromatics ($S_{C6–C8\ aromatics} = 12 \pm 4$ Cmol%) were evidenced over the catalysts under the conditions studied (Supporting Information, Table S1). The similar product distribution is consistent with the comparable active site quality, indicating that the lifetime differences derive from the quality of the pore structure. While some cycle times, such as the behavior of the samples alkaline treated for different times at fixed concentration (AT0.2-5 < AT0.2-10 < AT0.2-30), appear to simply relate to the increasing degree of mesoporosity, evidenced by N_2 sorption, Hg intrusion, and transmission electron microscopy (Table 1; Supporting Information, Figures S1 and S2), others are less straightforward to explain. In particular, the equivalent lifetime extensions (ca. 3.5 times that of C) displayed by zeolites treated for a fixed time at different concentrations (AT0.1-30 ≈ AT0.2-30 ≈ AT0.3-30) appear to be independent of the widely varying

[*] M. Milina, Dr. S. Mitchell, Prof. J. Pérez-Ramírez
ETH Zurich, Department of Chemistry and Applied Biosciences
Institute for Chemical and Bioengineering
Vladimir-Prelog-Weg 1, 8093 Zurich (Switzerland)
E-mail: jpr@chem.ethz.ch
Dr. D. Cooke, Dr. P. Crivelli
ETH Zurich, Department of Physics
Institute for Particle Physics
Otto-Stern-Weg 5, 8093 Zurich (Switzerland)

[**] This work was supported by the Swiss National Science Foundation (Project 200021-134572 and Ambizione grant PZ00P2-132059) and ETH Zurich (Grant ETH-47-12-1).

Supporting information for this article is available on the WWW under http://dx.doi.org/10.1002/anie.201410016.

Table 1: Composition, bulk porous and acidic properties, and pore connectivity of the ZSM-5 zeolites.

Sample	Si/Al [mol mol^{-1}]	V_{micro}[a] [cm^3 g^{-1}]	$V_{meso,N2}$[b] [cm^3 g^{-1}]	$V_{meso,Hg}$[c] [cm^3 g^{-1}]	S_{meso}[a] [m^2 g^{-1}]	d_{meso}[d] [nm]	$c_{Brønsted}$[e] [μmol g^{-1}]	c_{Lewis}[e] [μmol g^{-1}]	C_{pore}[f]
C	40	0.17	0.11	0.05	78	–	174	19	0.34
AT0.05-30	38	0.16	0.14	0.05	98	–	175	32	0.65
AT0.1-30	35	0.15	0.19	0.10	135	6	151	39	0.78
AT0.2-5	34	0.15	0.22	0.06	139	<4	150	49	0.45
AT0.2-10	30	0.14	0.30	0.10	205	5	145	52	0.56
AT0.2-30	25	0.12	0.39	0.25	272	8	147	78	0.83
AT0.3-30	21	0.09	0.72	0.49	376	13	146	75	0.80

[a] *t*-plot method. [b] $V_{meso,N2} = V_{total} - V_{micro}$. [c] Volume of Hg intruded in mesopores of 3.8–50 nm in diameter. [d] Average mesopore diameter from the BJH method. [e] IR study of adsorbed pyridine. [f] $C_{pore} = Ps_{vacuum}/Ps_{total}$ determined by PALS.

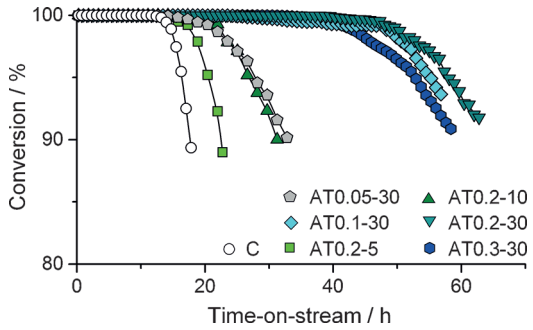

Figure 1. Conversion versus time-on-stream in the MTH reaction over the zeolites ($T = 723$ K, $P = 1$ bar, WHSV = 9.5 $g_{methanol}\, g_{zeolite}^{-1}\, h^{-1}$).

mesoporosity. This both indicates that despite being sensitive to differences in the pore structure the bulk textural parameters derived by these techniques are not suitable descriptors and has huge implications for the manufacturing efficiency of hierarchical zeolites as the amount of mesopores introduced directly relates to the yield of alkaline treatment (Supporting Information, Figure S3). A second striking observation is the huge difference in the performance of the zeolites prepared with shorter stronger or longer milder treatments (AT0.2-05 and AT0.1-30). Aside from a slightly smaller average mesopore size in the former (Supporting Information, Figure S2), these samples exhibit negligible differences in bulk porosity, suggesting that standard techniques are insensitive to subtleties in the pore structure which can appreciably impact the lifetime.

Clearly there is a need for better methods to optimize the design of zeolite catalysts. The recent addition of PALS to the characterization toolbox of hierarchical zeolites could contribute to the improved understanding of the pore topology.[6] In particular, the dynamic response of the annihilation of *ortho*-positronium (*o*-Ps) species formed upon positron implantation into the sample contains information about the pore connectivity.[8] If the pores are accessible to the external surface, *o*-Ps species can escape into vacuum, decaying with a characteristic lifetime of 142 ns. Otherwise, they may become entrapped within the material where, owing to the increased probability of surface collisions, the lifetime reduces with decreasing pore size. Thus, the fraction of the total amount of *o*-Ps formed which is emitted into vacuum offers a direct measure of the global pore connectivity ($C_{pore} = Ps_{vacuum}/Ps_{total}$) in the hierarchical zeolites (Tables 1; Supporting Information, Table S2). Remarkably, this parameter is found to excellently describe the MTH lifetime of all of the zeolites (Figure 2), including that of the previously reported system with constricted mesopores (AT0.2-TPA-30).[6]

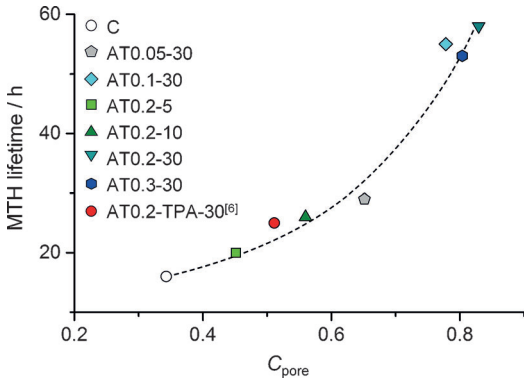

Figure 2. Correlation between the MTH lifetime of the zeolites and the global pore connectivity.

The equivalent pore connectivity determined by PALS and the plateauing dependence of the MTH lifetime with the mesopore volume and yield of zeolites prepared with different NaOH concentrations at longer treatment times (Figure 3a,b), point toward a critical mesopore size above which further enlargement no longer benefits the removal of coke precursors during the reaction. Analysis of the porosity of the catalysts at the end of the cycle (Supporting Information, Table S3) corroborates this hypothesis; the higher mesopore volume retained in the spent AT0.3-30 zeolite compared to AT0.1-30, indicating that this zeolite is excessively dissolved as the additional porosity does not contribute to an improved coke tolerance. On the other hand, the distinct pore connectivity and performance of zeolites of equivalent mesoporosity (AT0.2-5 and AT0.1-30) prepared with shorter concentrated or longer mild treatments are tentatively ascribed to differences in the mechanism of mesopore formation. Under the former conditions, the smaller nascent mesopores develop most prominently along grain boundaries of the zeolite crystals, which appear comparatively pristine (Figure 3c; Supporting Information, Figure S4). In contrast,

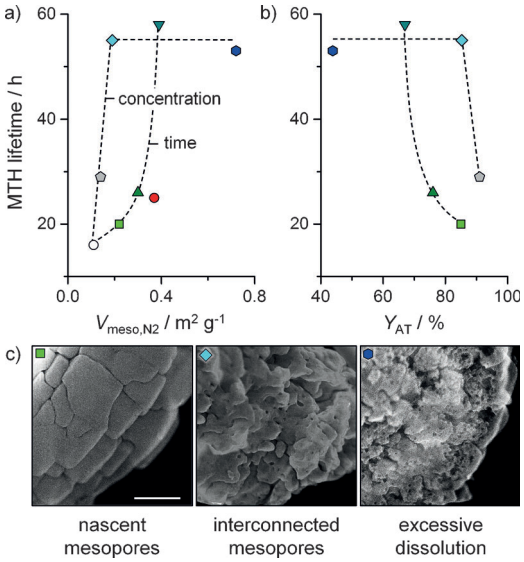

Figure 3. Correlation between the MTH catalyst lifetime and a) the mesopore volume and b) the yield of alkaline treatment. c) Scanning electron micrographs exposing the distinct mesopore structure of hierarchical zeolites prepared by alkaline treatment for different time or concentration. See Figure 2 for legend. Scale bar in (c): 100 nm (applies to all images).

prolonged treatments appear to favor the more directed development of larger interconnected and intracrystalline mesopores, which enhance the active site accessibility. Distinct modes of mesopore formation by desilication have been previously postulated to originate from differences in the zeolite composition and particle morphology,[9] but our results show that the treatment conditions also have a strong impact.

In summary, we have demonstrated the unprecedented sensitivity of PALS to the impact of subtle differences in the pore structure which govern the tolerance of hierarchical zeolites to coking in hydrocarbon transformations. This exceptional ability can be attributed to the extremely short temporal probing window of positronium to the pore network compared with most other techniques of porosity assessment. Advantageously, the pore connectivity derived requires no parameterization and thus, unlike other common porosity variables, is not influenced by prior assumptions about the geometry, surface interactions, and so on. Furthermore, the technique is not limited to the analysis of powders; the equivalent global connectivity evidenced for AT0.2-30 following extrusion with a kaolin binder confirmed that the interaction between the component phases did not hinder the escape of *o*-Ps owing to pore blockage (Supporting Information, Table S1). However, as the lifetime of *o*-Ps in large pores (for example, more than 100 nm in diameter) becomes comparable to the value in vacuum, the connectivity of the macropore network in shaped bodies cannot be directly extracted from the PALS spectra. In this case, the amount of *o*-Ps decaying within large interparticle voids could be determined by the simultaneous application of a time-of-flight (TOF) detector. Thus, the application of PALS, which is currently unexplored in catalysis, opens new doors for the improved design of diverse porous materials over a wide range of length scales.

Experimental Section

Alkaline treatments of the conventional ZSM-5 zeolite (CBV 8014, Zeolyst International) were performed in stirred 0.05–0.3 M NaOH solutions (30 $cm^3 g_{zeolite}^{-1}$) at 338 K for 5–30 min. All samples were converted into protonic form by three consecutive ion exchanges in an aqueous NH_4NO_3 solution (0.1 M, 298 K, 8 h, 100 $cm^3 g_{zeolite}^{-1}$) and calcined at 823 K (5 K min^{-1}) for 5 h prior to characterization and catalytic evaluation. Extrudates (4 mm diameter) were obtained by shaping AT0.2-30 zeolite with a kaolin binder (20 wt.%) followed by drying and calcination at 873 K for 5 h (5 K min^{-1}). The catalysts were characterized by inductively coupled plasma optical emission spectroscopy, nitrogen sorption, Fourier-transform infrared spectroscopy of adsorbed pyridine, transmission and scanning electron microscopy, and positron annihilation lifetime spectroscopy. The methanol-to-hydrocarbons reaction was carried out in a fixed-bed reactor at 723 K using a weight hourly space velocity (WHSV) of 9.5 $g_{methanol}\, g_{zeolite}^{-1} h^{-1}$ coupled with online GC analysis. Characterization and testing procedures are fully detailed in the Supporting Information.

Received: October 13, 2014
Published online: November 5, 2014

Keywords: heterogeneous catalysis · methanol-to-hydrocarbons · pore connectivity · positron annihilation lifetime spectroscopy · zeolites

[1] a) V. Karageorgiou, D. Kaplan, *Biomaterials* **2005**, *26*, 5474 – 5491; b) D. M. D'Alessandro, B. Smit, J. R. Long, *Angew. Chem. Int. Ed.* **2010**, *49*, 6058 – 6082; *Angew. Chem.* **2010**, *122*, 6194 – 6219; c) X. Zhao, J. Kim, C. A. Cezar, N. Huebsch, K. Leeb, K. Bouhadird, D. J. Mooney, *Proc. Natl. Acad. Sci. USA* **2011**, *108*, 67 – 72; d) N. Tétreault, M. Grätzel, *Energy Environ. Sci.* **2012**, *5*, 8506 – 8516; e) S. Dutta, A. Bhaumik, K. C.-W. Wu, *Energy Environ. Sci.* **2014**, *7*, 3574 – 3592.

[2] a) M. Hartmann, *Angew. Chem. Int. Ed.* **2004**, *43*, 5880 – 5882; *Angew. Chem.* **2004**, *116*, 6004 – 6006; b) L. Tosheva, V. P. Valtchev, *Chem. Mater.* **2005**, *17*, 2494 – 2513; c) M. Choi, H. S. Cho, R. Srivastava, C. Venkatesan, D.-H. Choi, R. Ryoo, *Nat. Mater.* **2006**, *5*, 718 – 723; d) J. Pérez-Ramírez, C. H. Christensen, K. Egeblad, C. H. Christensen, J. C. Groen, *Chem. Soc. Rev.* **2008**, *37*, 2530 – 2542; e) S. Lopez-Orozco, A. Inayat, A. Schwab, T. Selvam, W. Schwieger, *Adv. Mater.* **2011**, *23*, 2602 – 2615; f) K. Na, C. Jo, J. Kim, K. Cho, J. Jung, Y. Seo, R. J. Messinger, B. F. Chmelka, R. Ryoo, *Science* **2011**, *333*, 328 – 332; g) W. J. Roth, O. V. Shvets, M. Shamzhy, P. Chlubná, M. Kubů, P. Nachtigall, J. Čejka, *J. Am. Chem. Soc.* **2011**, *133*, 6130 – 6133; h) D. P. Serrano, J. M. Escola, P. Pizarro, *Chem. Soc. Rev.* **2013**, *42*, 4004 – 4035; i) W. J. Roth, P. Nachtigall, R. E. Morris, J. Čejka, *Chem. Rev.* **2014**, *114*, 4807 – 4837; j) P. S. Wheatly, P. Chlubná-Eliášová, H. Greer, W. Zhou, V. R. Seymour, D. M. Dawson, S. E. Ashbrook, A. B. Pinar, L. B. McCusker, M. Opanasenko, J. Čejka, R. E. Morris, *Angew. Chem. Int. Ed.* **2014**, DOI: 10.1002/anie.201407676; *Angew. Chem.* **2014**, DOI: 10.1002/ange.201407676.

[3] a) J. Zečević, C. J. Gommes, H. Friedrich, P. E. de Jongh, K. P. de Jong, *Angew. Chem. Int. Ed.* **2012**, *51*, 4213 – 4217; *Angew. Chem.* **2012**, *124*, 4289 – 4293; b) J. M. Thomas, R. K. Leary, *Angew. Chem. Int. Ed.* **2014**, *53*, 12020 – 12021; *Angew. Chem.* **2014**, *126*, 12214 – 12215.

[4] a) S. Mitchell, N.-L. Michels, K. Kunze, J. Pérez-Ramírez, *Nat. Chem.* **2012**, *4*, 825 – 831; b) B. M. Weckhuysen, *Angew. Chem. Int. Ed.* **2009**, *48*, 4910 – 4943; *Angew. Chem.* **2009**, *121*, 5008 – 5043.
[5] a) K. Cho, H. S. Cho, L.-C. Menorval, R. Ryoo, *Chem. Mater.* **2009**, *21*, 5664 – 5673; b) J. Kärger, R. Valiullin, *Chem. Soc. Rev.* **2013**, *42*, 4172 – 4197; c) Q. Wang, et al., *RSC Adv.* **2014**, *4*, 21479 – 21491.
[6] M. Milina, S. Mitchell, P. Crivelli, D. Cooke, J. Pérez-Ramírez, *Nat. Commun.* **2014**, *5*: 3922 DOI: 10.1038/ncomms4922.
[7] J. Pérez-Ramírez, S. Mitchell, D. Verboekend, M. Milina, N.-L. Michels, F. Krumeich, N. Marti, M. Erdmann, *ChemCatChem* **2011**, *3*, 1731 – 1734.
[8] a) D. W. Gidley, H. G. Peng, R. S. Vallery, *Annu. Rev. Mater. Res.* **2006**, *36*, 49 – 79; b) D. W. Gidley, W. E. Frieze, T. L. Dull, A. F. Yee, E. T. Ryan, H.-M. Ho, *Phys. Rev. B* **1999**, *60*, 5157 – 5160.
[9] S. Svelle, L. Sommer, K. Barbera, P. N. R. Vennestrøm, U. Olsbye, K. P. Lillerud, S. Bordiga, Y.-H. Pan, P. Beato, *Catal. Today* **2011**, *168*, 38 – 47.

